Structural Engineering and Mechanics, Vol. 15, No. 5 (2003) 563-578
DOI: http://dx.doi.org/10.12989/sem.2003.15.5.563

Adaptive finite elements by Delaunay triangulation for fracture analysis of cracks

Pramote Dechaumphai† and Sutthisak Phongthanapanich‡

Mechanical Engineering Department, Chulalongkorn University, Bangkok 10330, Thailand

Paritud Bhandhubanyong‡†

National Metal and Materials Technology Center, Bangkok 10400, Thailand

(Received May 20, 2002, Accepted March 14, 2003)

Abstract. Delaunay triangulation is combined with an adaptive finite element method for analysis of two-dimensional crack propagation problems. The content includes detailed descriptions of the proposed procedure which consists of the Delaunay triangulation algorithm and an adaptive remeshing technique. The adaptive remeshing technique generates small elements around the crack tips and large elements in the other regions. Three examples for predicting the stress intensity factors of a center cracked plate, a compact tension specimen, a single edge cracked plate under mixed-mode loading, and an example for simulating crack growth behavior in a single edge cracked plate with holes, are used to evaluate the effectiveness of the procedure. These examples demonstrate that the proposed procedure can improve solution accuracy as well as reduce total number of unknowns and computational time.

Key words: adaptive mesh; Delaunay triangulation; finite element method; stress intensity factors; crack propagation.

1. Introduction

Domain discretization into a number of elements is the first step in the finite element analysis. Due to the ever increasing complexity of the domains, new improved general-purpose mesh generation algorithms have been in high demand. The Delaunay triangulation, based on the concept of the Voronoi diagram (Bowyer 1981, Watson 1981), is one of the automated mesh generation algorithms that has recently gained popularity. The algorithm can generate mesh of arbitrary geometry for both simply connected and multi-boundary domains. The procedure that is capable of generating mesh with proper nodal density and regularity of the triangulation for arbitrary two-dimensional geometry was first introduced by Weatherill and Hassan (1994) and revised by Karamete *et al.* (1997). In this paper, the Delaunay triangulation which constructs triangular mesh for crack propagation analysis is described in details. In addition, an adaptive remeshing technique

† Professor, Graduate Program Director
‡ Graduate Student
‡† Director

is developed and incorporated into the Delaunay triangulation in order to improve the solution accuracy of the finite element method. The technique generates an entirely new mesh based on the solution obtained from the previous mesh; such that elements in regions with large changes of solution gradients become smaller and elements in areas with little changes of solution gradients grow larger.

For crack propagation problems, the stress intensity factor is a critical parameter in the prediction of fatigue crack growths. The standard six-node isoparametric elements are used in the finite element models in this study. In order to improve the accuracy of the near-tip stress fields, elements with mid-side nodes displaced from their nominal positions to quarter points are employed near the crack tip (Barsoum 1977). The nodal displacements around the crack tip are then used to determine the stress intensity factors using the displacement extrapolation method (Chan *et al.* 1970). In this paper, several examples under mode I and II loadings are modeled to evaluate the effectiveness of the combined procedure. In addition, the capability of the proposed procedure is further demonstrated by the simulation of the crack propagation trajectory in a single edge cracked plate with holes under mixed-mode loading.

2. Formulation

2.1 Stress intensity factor and crack propagation

The stress intensity factors (Anderson 1991) designated as K_I and K_{II} for the fracture modes I and II, representing the opening and shearing mode, respectively, may be determined from (Chan *et al.* 1970, Guinea *et al.* 2000),

$$K_I = \frac{E}{3(1+\nu)(1+\kappa)}\sqrt{\frac{2\pi}{L}}\left(4(v_b - v_d) - \frac{(v_c - v_e)}{2}\right) \tag{1a}$$

$$K_{II} = \frac{E}{3(1+\nu)(1+\kappa)}\sqrt{\frac{2\pi}{L}}\left(4(u_b - u_d) - \frac{(u_c - u_e)}{2}\right) \tag{1b}$$

where E is the modulus of elasticity, ν is the Poisson's ratio, κ is the elastic parameter defined by $(3 - 4\nu)$ for plane strain and $(3 - \nu)/(1 + \nu)$ for plane stress problems, and L is the element length. The u and v are respectively the displacement components in the x and y directions; their subscripts indicate the position as shown in Fig. 1.

Crack propagation in practical problems normally occurs under mixed mode loading. Based on the maximum circumferential stress theory (Erdogan and Sih 1963), the direction of crack propagation θ may be computed from,

$$K_I \sin\theta + K_{II}(3\cos\theta - 1) = 0 \tag{2}$$

For the pure mode I loading, Eq. (2) implies that the crack propagates at zero angle θ. But for mixed mode loading, the crack propagates at non-zero angle θ as depicted in Fig. 2. The quarter-point six-node elements (Barsoum 1977) as shown in Fig. 3 are used in this work to form up a circular zone surrounding the crack tip. The radius of the circular zone is specified to be no larger than one-eight of the initial crack length, and with roughly one element every 30 degrees in the circumferential direction (Guinea *et al.* 2000). The increment of the crack length during each crack

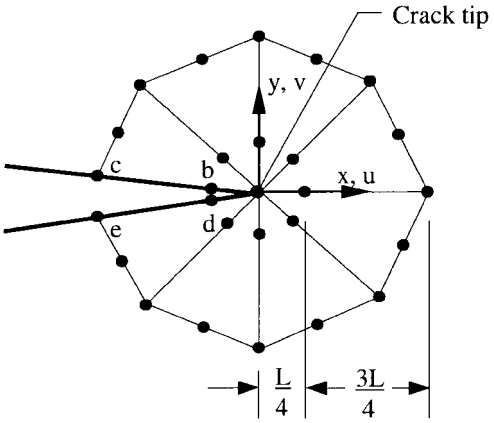

Fig. 1 Quarter-point triangular elements around the crack tip

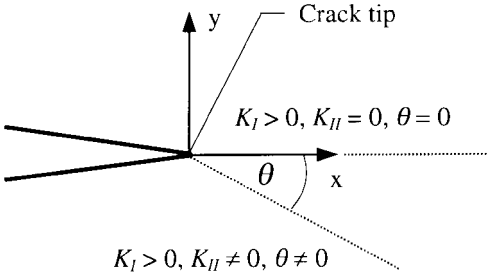

Fig. 2 Angle of crack trajectory

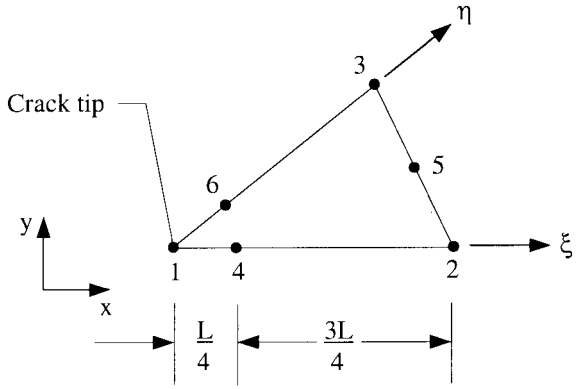

Fig. 3 Quarter-point six-node triangular element

propagation step is specified by the user. With Delaunay triangulation capability described in the following section and the presence of the crack geometry, a new mesh can be generated according to the new geometry automatically.

2.2 Finite element equations

Finite element equations for determining nodal displacements and stresses can be derived from the governing partial differential equations that represent the equilibrium conditions (Zienkiewicz and Taylor 2000). These equations can be written in matrix form as,

$$[K]\{\delta\} = \{F\} \tag{3}$$

where $\{\delta\}$ is the vector that contains unknowns of the element nodal displacements, $\{F\}$ is the load vector, and $[K]$ is the stiffness matrix given by,

$$[K] = \int_A [B]^T [C][B] t\, dA \tag{4}$$

In the above Eq. (4), $[B]$ is the strain-displacement matrix, $[C]$ is the material stiffness matrix that depends on the condition of plane stress or plane strain, t is the element thickness, and A is the element area. Element equations (3) with appropriate boundary conditions are evaluated for each element before assembling them together to form up a set of system equations prior to solving for all nodal displacements.

3. Delaunay triangulation for crack propagation analysis

3.1 Concept

Dirichlet (Bowyer 1981, Watson 1981) proposed a method to construct Dirichlet tessellation or Voronoi diagram, for which a domain could be decomposed into a set of packed convex polygons. For a given set of points in space, $\{P_k\}$, $k = 1, \ldots, n$, the regions $\{V_k\}$, $k = 1, \ldots, n$, are boundaries assigned to each point P_k and represent the space closer to P_k than to any other points in the set. Therefore, these regions satisfy,

$$V_k = \{P_i: |p - P_i| < |p - P_j|, \forall j \neq i\} \tag{5}$$

If all points which have some segments of a Voronoi boundary in common are joined, the resulting shape is a Delaunay triangulation as shown in Fig. 4. In graph theory, the characteristic of Delaunay triangulation can be defined such that the graph which any circle in the plane is said to be empty if it contains no vertex in its interior. This defining characteristic of the Delaunay triangles is called the empty circumcircle property.

3.2 Mesh generation procedure

The Delaunay triangulation algorithm based on the in-circle criterion was initiated by Bowyer (1981). The algorithm was then extended and applied to an unsteady high-speed compressible flow analysis (Phongthanapanich and Dechaumphai 2002). In this paper, the algorithm is extended to crack propagation analysis with special isosceles six-node triangles around the crack tip. The key idea of the algorithm is summarized in the algorithm I below;

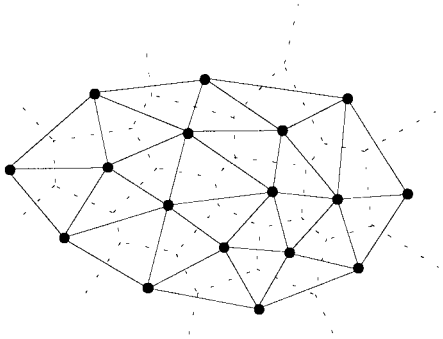

Fig. 4 Delaunay triangulation dual of Voronoi diagram for a given set of points

Algorithm I; Delaunay Triangulation

1. Let P, $k = 1, \ldots, n$, be the set of nodes on the boundaries of domain that stored in sequence of counter-clockwise direction for all outside boundaries and clockwise direction for all inside boundaries. Let T be the empty set of Delaunay triangles.
2. Search crack tip nodes from the set P and their two adjacent nodes. Remove crack tip nodes from the set P and mark the position of those nodes in the set P for the next operation.
3. Create rosette nodes around crack tips as shown in Fig. 5 with the specified angle and store in set P by insertion at the location that marked at step 2. These nodes are stored in clockwise direction sequence for outside boundary crack tip and counter-clockwise direction sequence for inside boundary crack tip.
4. Create an initial convex hull triangle that contains all boundary nodes inside. Add the triangle to T.
5. Read next boundary node p_i from P.
6. Search triangle t_i in T which contains the node p_i inside. The search starts from the triangle which was formed last and uses Lawson's algorithm (Lawson 1977, Sloan 1993) to march from one triangle to the next in the direction of p_i. This algorithm performs the shortest path searching strategy and removes the need to search through the entire domain.
7. Destroy surrounding triangles of t_i which lie within a circle centered at a vertex of the Voronoi diagram. Delete these triangles from T. Then form new triangles that connected to the node p_i. These triangles must pass the in-circle criterion. Add new forming triangles into T and determine the neighboring triangles of the triangles.
8. Go to step 5 until all nodes in P are considered.
9. Search for all triangles that have one or more vertices connected to any vertices of initial convex hull triangles outside the domain or lie inside holes in the domain and delete these triangles from T.
10. Add crack tip nodes in to the domain at the specified position and create rosette elements by connecting all rosette nodes to the crack tip nodes.

3.3 Automatic node creation procedure

The Delaunay triangulation algorithm described above does not explain the method for creating new nodes inside the domain. So far, researchers have introduced several approaches for creating

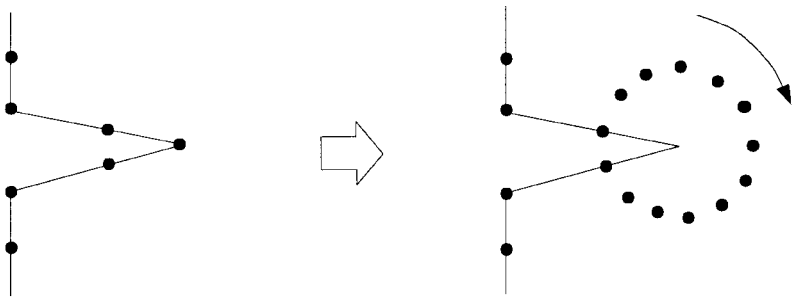

Fig. 5 Removal of the crack tip node and creation of rosette nodes around the crack tip

new nodes inside the domain by refining boundary triangles such that the set of boundary points guide new node placements (Frey 1987, Borouchaki and George 1997). The new node creation procedure for geometry with crack developed in this paper is extended from that proposed by Weatherill and Hassan (1994), and Karamete *et al.* (1997). The shape and size of triangles or density of nodes inside the domain are controlled by two coefficients, the Alpha and the Beta coefficients. The Alpha coefficient controls node density by changing the allowable shape of the formed triangles. The Beta coefficient controls the regularity of triangulation by disallowing node within a specified distance of each other to be inserted in the same sweep of the triangles within the field. The suggested values of both the Alpha and the Beta coefficients for coarse and fine triangular meshes are 0.8 and 0.9, and 0.5 and 0.6 respectively.

The main idea of the automatic node creation procedure is the search for the triangle that conforms with both Alpha and Beta testing criteria and a new node placement at the centroid of that triangle. New triangles can then be created by Delaunay triangulation algorithm as described in algorithm I. The detailed implementation of the automatic node creation procedure is described in algorithm II as follows.

Algorithm II; Mesh Refinement

1. Let P, $k = 1, \ldots, n$, be the set of nodes on the boundaries of domain that stored in sequence of counter-clockwise direction for all outside boundaries and clockwise direction for all inside boundaries.
2. Let V be the empty set of new inserted nodes and let T be the set of Delaunay triangles which constructed from algorithm I.
3. Compute the nodal distribution value dp_i for each boundary nodes p_i by,

$$dp_i = \frac{1}{M}\sum_{j=1}^{M} |p_j - p_i| \tag{6}$$

   where $|\ |$ is the Euclidean distance assuming that node i is surrounded by M nodes (see Fig. 6).
4. Read triangle t_i from T.
5. If one vertex of this triangle is connected to any crack tip node then go to step 4 to read the next triangle.
6. Calculate centroid of the triangle t_i and define as node Q, then compute the nodal distribution value of node Q by using Eq. (6). Compute the distance d_m, $m = 1, 2, 3$, from node Q to each of the three vertices of the triangle t_i.
7. Perform the Alpha test for node Q.
   If $d_m < (\alpha\, dp_q)$ for any $m = 1, 2, 3$, then reject the node Q and go to step 4.
8. Compute the distance s_j for any $j = 1, \ldots, N$ from node Q to be inserted to the other nodes.
9. Perform the Beta test for node Q.
   If $s_j < (\beta\, dp_q)$ for any $j = 1, ..., N$, then reject the node Q and go to step 4.
10. Accept the node Q for insertion by the Delaunay triangulation algorithm (Algorithm I). Assign the interpolated value of the nodal distribution value to the new node Q and add node Q into V.
11. Go to step 4 until all triangles in T are considered.
12. Perform the Delaunay triangulation of the derived nodes in V by Algorithm I.

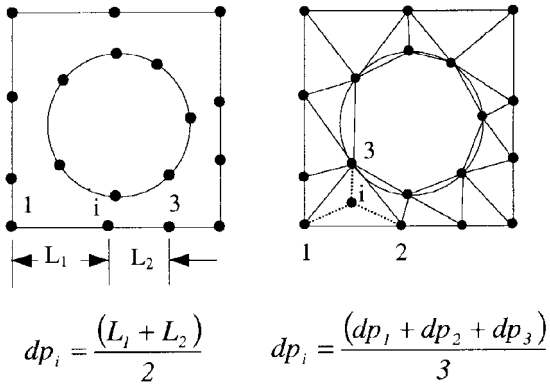

Fig. 6 Calculation of the nodal distribution values

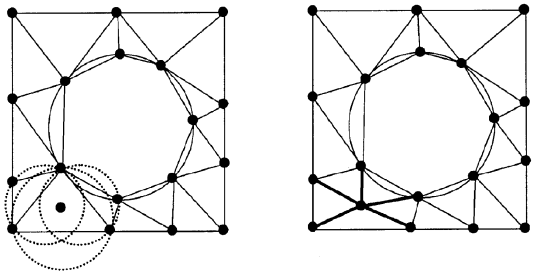

Fig. 7 Mesh refinement with automatic node creation scheme (Algorithm II)

A demonstration of a domain refinement by creating a new node inside the domain by Algorithm I and II is shown in Fig. 7. The new node that conforms with both the Alpha and Beta testing criteria is inserted at the centroid of the triangle and the in-circle testing criterion is applied to all neighborhood triangles. With this process, a new mesh with refined triangles is formed.

3.4 Mesh smoothing

Shapes and sizes of triangles formed from the previous step can be improved by applying a mesh smoothing technique. This paper uses the Laplacian smoothing technique because of less computational time requirement. The point repositioning formula is derived from the finite difference approximation of the Laplace's equation (Frey 1987). Each interior node is moved successively to the centroid of the area which is formed by connecting neighbouring nodes. Several passes are made through the entire set of all interior nodes to produce optimized shape and size of the triangles. The new node locations using the Laplacian smoothing are computed from,

$$x_{ic} = \frac{\sum_{i=1}^{M} x_i}{M} \quad \text{and} \quad y_{ic} = \frac{\sum_{i=1}^{M} y_i}{M} \qquad i = 1, 2, \ldots, M \tag{7}$$

where x_i and y_i are the coordinates of the surrounding M nodes.

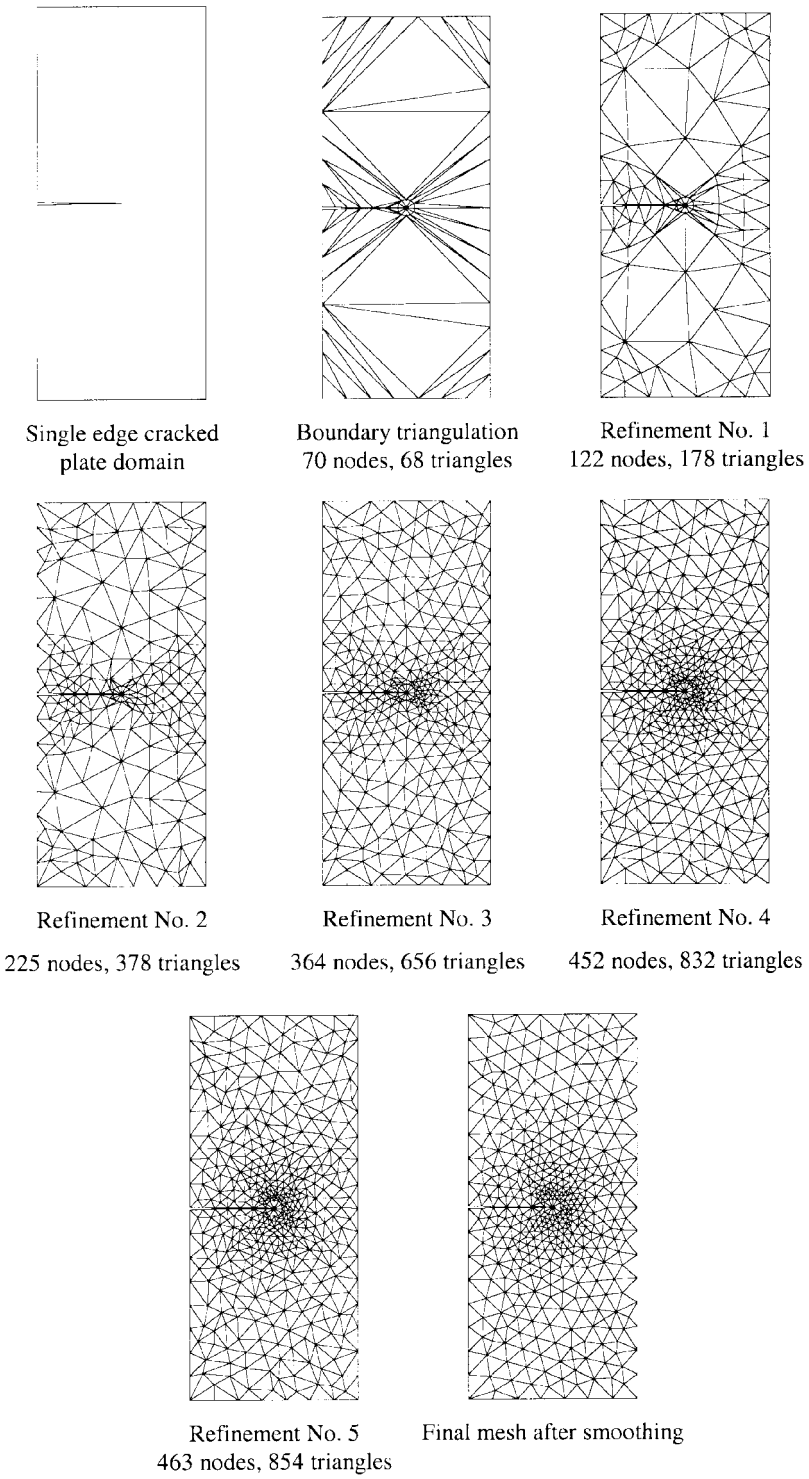

Fig. 8 Mesh refinement and smoothing for the single edge cracked plate

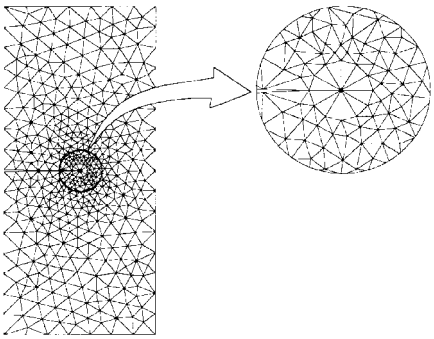

Fig. 9 Rosette triangular elements around the crack tip of the single edge cracked plate

To demonstrate the efficiency of the Delaunay triangulation algorithm and the Laplacian smoothing technique, Fig. 8 shows the progress of the domain discretization refinement for the single edge cracked plate. The geometry consists of a horizontal crack line on the left boundary of the domain. Fig. 9 shows detailed rosette triangular elements around the crack tip constructed by the above algorithms.

4. Adaptive remeshing technique

The remeshing technique generates an entirely new mesh based on the solution obtained from a previous mesh. The technique was first introduced and applied for high-speed compressible flow analysis (Peraire *et al.* 1987). In this paper, the technique is modified and corporated into the Delaunay triangulation and the finite element method to analyze crack propagation problems. There are two main steps in the implementation of the adaptive remeshing technique; the first step is the determination of proper element sizes and the second step is the new mesh generation.

4.1 Element sizes determination

The von Mises stress σ is used as the indicator for computing proper element sizes at different locations in the domain (Dechaumphai 1996). As small elements must be placed in the region where changes in the von Mises stress gradients are large, the second derivatives of the von Mises stress at a point with respect to global coordinates x and y are needed. Using the concept of principal stresses determination from a given state of stresses at a point, the principal quantities in the principal directions X and Y where the cross-derivatives vanish are determined,

$$\begin{bmatrix} \dfrac{\partial^2\sigma}{\partial x^2} & \dfrac{\partial^2\sigma}{\partial x\partial y} \\ \dfrac{\partial^2\sigma}{\partial x\partial y} & \dfrac{\partial^2\sigma}{\partial y^2} \end{bmatrix} \Rightarrow \begin{bmatrix} \dfrac{\partial^2\sigma}{\partial X^2} & 0 \\ 0 & \dfrac{\partial^2\sigma}{\partial Y^2} \end{bmatrix} \tag{8}$$

The maximum principal quantities are then used to compute the proper element size h_i by requiring that the error should be uniform for all elements,

$$h_i^2\lambda_i = h_{\min}^2\lambda_{\max} = constant \tag{9}$$

where λ_i is the higher principal quantity of the element considered,

$$\lambda_i = \max\left(\left|\frac{\partial^2 \sigma}{\partial X^2}\right|, \left|\frac{\partial^2 \sigma}{\partial Y^2}\right|\right) \tag{10}$$

In Eq. (9), λ_{max} is the maximum principal quantity for all elements and h_{min} is the minimum element size specified by users.

4.2 Adaptive mesh regeneration

The proposed adaptive mesh regeneration is based on the concepts of the Delaunay triangulation and the mesh refinement as described by Algorithm I and II. The new mesh is constructed using the information from the previous mesh (background mesh), such that it consists of small elements in the regions with large changes in solution gradients, and large elements in the other regions where the changes in solution gradients are small. Detailed process of the adaptive remeshing technique is described in algorithm III as follows.

Algorithm III; Adaptive Remeshing

1. Let *P*, k = 1, …, n be the set of nodes of the background mesh. Let *T*, l = 1, …, m be the set of triangles of the background mesh.
2. Let *NP* be the empty set of nodes and *NT* be the empty set of triangles.
3. Calculate the new proper element size h_i of all the nodes of the background mesh by Eqs. (8) and (9). Then rediscretize all boundaries of the domain based on the new proper elements size h_i and recompute the nodal distribution values dp_i for all the boundary nodes before adding all nodes into *NP*.
4. Obtain nodal values of the new mesh by interpolating the nodal values of the background mesh. Construct boundary triangles from the new boundary nodes in *NP* by Algorithm I and store all the new triangles into *NT*.
5. Refine the boundary triangles based on the given values of the Alpha and Beta coefficients by Algorithm II and store all new inserted nodes into *NP*.
6. Read next interior node p_i of the background mesh from *P*.
7. If $h_i > h_{max}$ then go to step 6.
8. Search triangle t_i in *NT* which contains the node p_i using the method described in step 6 of Algorithm I. Then calculate the centroid of the triangle t_i and define as node *Q*, and compute the nodal distribution value of node *Q* by Eq. (6).
9. Compute the distance d_m, m = 1, 2, 3, from node *Q* to each of the three vertices of the triangle t_i.
10. If h_i > average of d_m or $h_{min} > d_m$, m = 1, 2, 3 then go to step 6.
11. Otherwise accept the node *Q* for insertion by the Delaunay triangulation algorithm (Algorithm I). Assign the interpolated value of the nodal distribution value to the new node *Q* and add to *NP*.
12. Go to step 6 until all nodes in *P* are considered.
13. Perform the Delaunay triangulation of the inserted nodes in *NP* by Algorithm I and smooth the mesh.
14. Create mid-side nodes for all element sides and relocate all mid-side nodes of the crack tip elements to the quarter-point positions as shown in Fig. 1.

5. Algorithm evaluation

The fracture mechanics simulation with the finite element program is used to evaluate the efficiency of the combined Delaunay triangulation and the adaptive remeshing technique. The entire procedure is first used to determine the stress intensity factors for problems with analytical solutions or experimental data so that their results can be compared. The procedure is then employed to capture the crack trajectory by adapting the mesh automatically with the crack growth.

5.1 Determination of stress intensity factors

Three well-known geometries used in the evaluation of the proposed procedure are: (1) the center cracked plate, (2) the compact tension specimen, and (3) the single edge cracked plate under mixed-mode loading.

The center cracked plate: The geometry of the center cracked plate and its final adaptive mesh are shown in Fig. 10. The plate has an initial crack length $2a$ = 100 units, and the thickness t = 1 unit. The stress intensity factor for this problem was derived (Isida 1971) in closed-form as,

$$K_I = 1.334\sigma\sqrt{\pi a} \tag{11}$$

Both the full and a quarter models were used to analyze this problems. The computed stress intensity factor K_I from either model is 16.7611 comparing to 16.7192 from Eq. (11) with the difference of 0.25%.

The compact tension specimen: The geometry of the compact tension specimen and its final adaptive mesh are shown in Fig. 11. The specimen has an initial crack length a = 3 mm., the width w = 50.8 mm., and the thickness t = 25.4 mm. The closed-form formula for the stress intensity factor (ASTM 1996) is,

$$K_I = P\left(2+\frac{a}{w}\right)\left(0.886+4.64\left(\frac{a}{w}\right)-13.32\left(\frac{a}{w}\right)^2+14.72\left(\frac{a}{w}\right)^3-5.6\left(\frac{a}{w}\right)^4\right)\Big/ t\sqrt{w}\left(1-\frac{a}{w}\right)^{\frac{3}{2}} \tag{12}$$

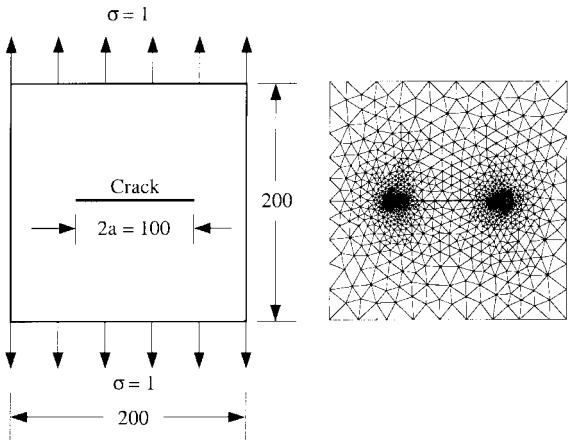

Fig. 10 Problem statement and the final mesh of the center cracked plate

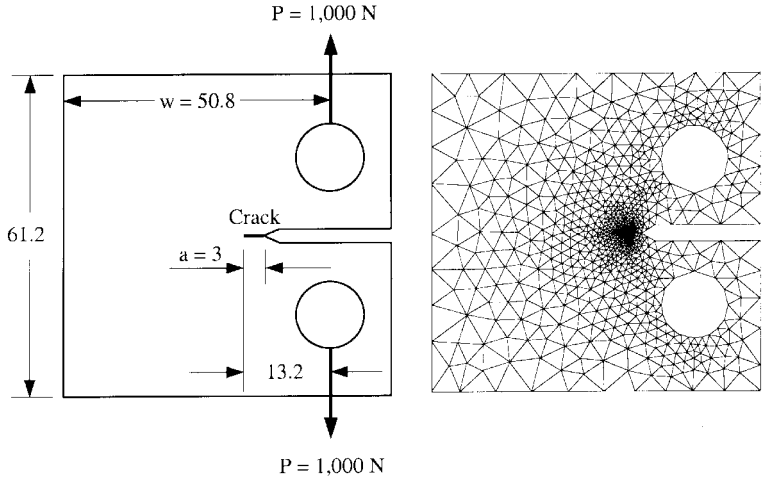

Fig. 11 Problem statement and the final mesh of the compact tension specimen

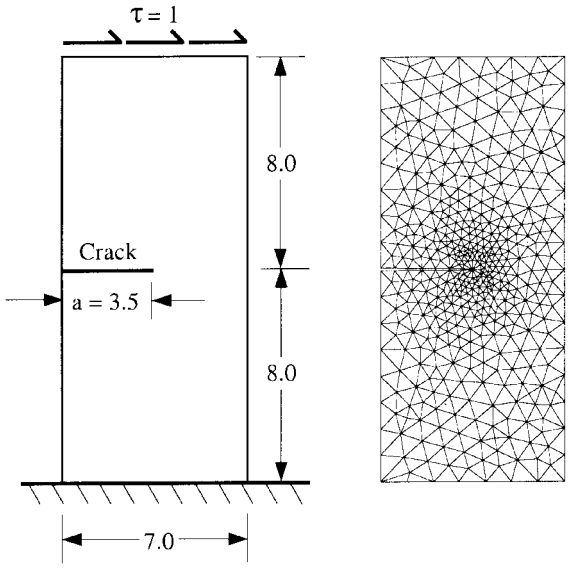

Fig. 12 Problem statement and the final mesh of the single edge cracked plate under mixed-mode loading

The computed stress intensity factor from the adaptive model as shown in Fig. 11 is 27.718 comparing to 27.935 from Eq. (12) with the difference of 0.75%.

The single edge cracked plate under mixed-mode loading: The geometry of the single edge cracked plate and its final adaptive mesh are shown in Fig. 12. The plate has an initial crack length a = 3.5 units. The computed stress intensity factors K_I and K_{II} from the adaptive mesh shown are 34.10 and 4.52 comparing to the reference values of 34.00 and 4.55 (Rao and Rahman 2000) with the differences of 0.3% and 0.7%, respectively.

5.2 Simulation of crack growth trajectory

Fig. 13 describes the flow-chart for predicting the crack growth trajectory of a single edge cracked plate with holes under mixed-mode loading. The single edge cracked plate with dimensions as shown in Fig. 14 has three small holes on it. The plate is simply supported near the lower corners, and is subjected to a concentrated load at the center of the upper edge. This problem was carried out using the experiment by Bittencourt *et al.* (1996) with two cases of the initial crack length, *a*, and its location, *b*, as shown by the table in Fig. 14. For the first case, the initial crack length, *a*, and its location, *b*, are 1.5 and 5.0 units, respectively. The results of the adaptive finite element meshes and the crack growth trajectory are depicted in Fig. 15. The figure shows that the crack

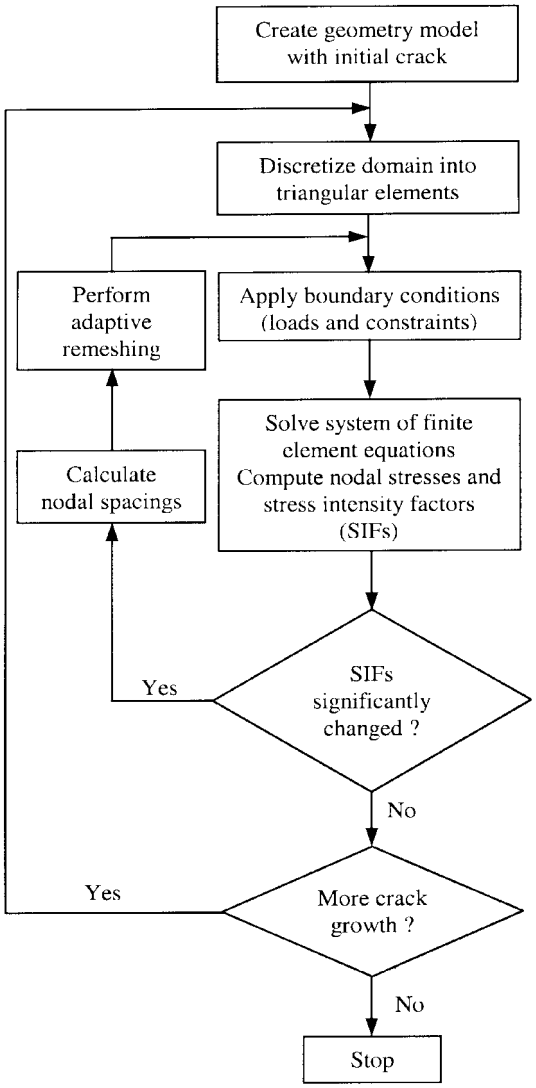

Fig. 13 Flow-chart for predicting crack growth trajectory

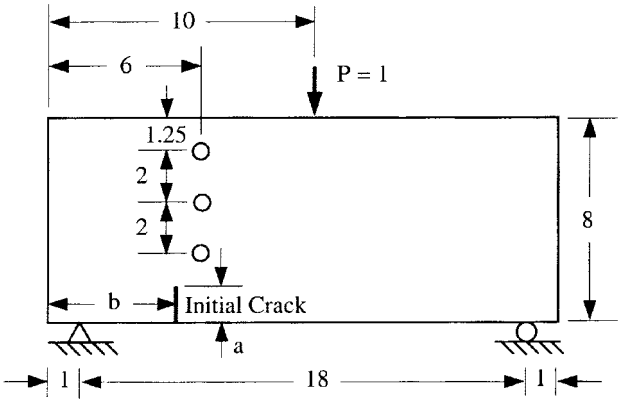

Specimen	a	b
Case I	1.5	5.0
Case II	1.0	4.0

Fig. 14 Problem statement for the single edge crack plate with holes

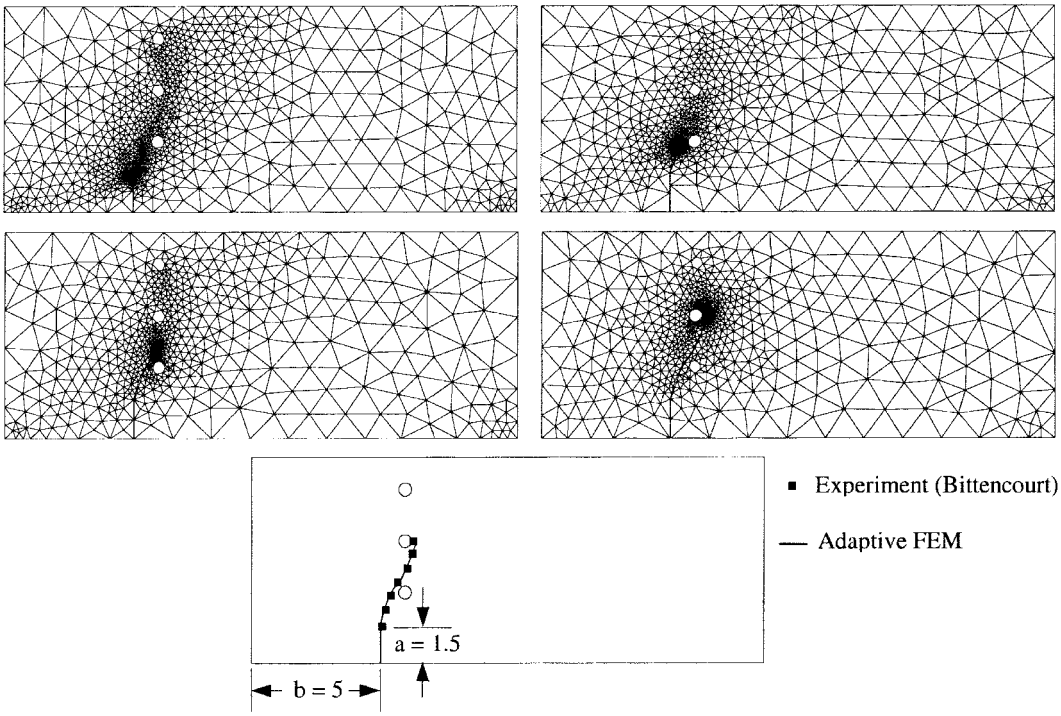

Fig. 15 Adaptive finite element meshes and the crack growth trajectory for the single edge cracked plate with holes under mixed-mode loading (Case I)

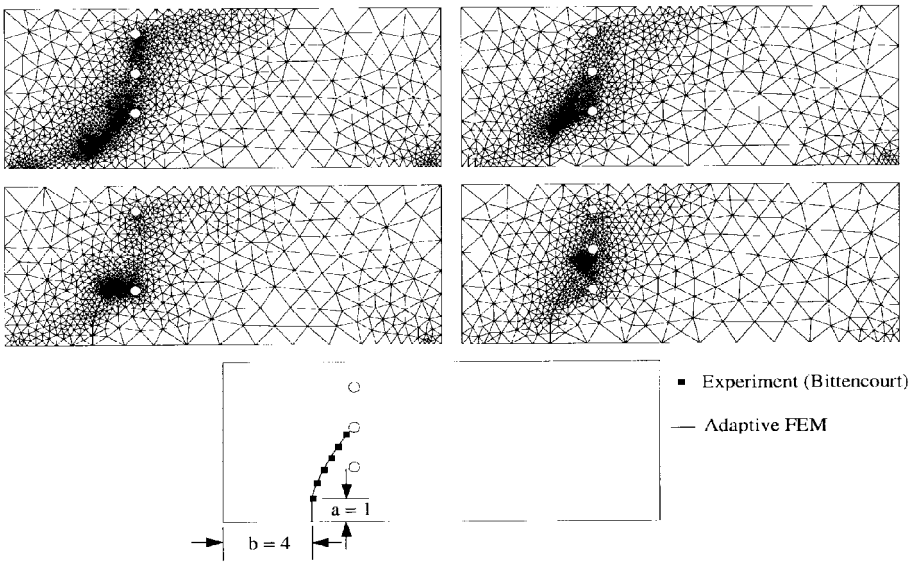

Fig. 16 Adaptive finite element meshes and the crack growth trajectory for the single edge cracked plate with holes under mixed-mode loading (Case II)

growth trajectory passes near the lower hole and ended at the middle hole. Fig. 16 shows the similar result but for the second case with the initial crack length, *a*, and its location, *b*, of 1.0 and 4.0, respectively. For this latter case, the crack propagates toward the middle hole. The crack growth trajectories for these two cases resemble very well with the experimental results.

6. Conclusions

The adaptive finite element method using Delaunay triangulation for crack propagation analysis was presented. The concept of the Delaunay triangulation for two-dimensional mesh construction was explained. The mesh generation procedure with automatic node creation and mesh smoothing were described in details. The technique was combined with the finite element method for analyzing crack problems under single and mixed mode loadings. The isoparametric six-node triangular elements, with mid-side nodes displaced from their nominal positions to quarter points of the crack tip, were employed to form up a circular zone surrounding the crack tip in order to increase solution accuracy.

The solution accuracy was further improved by implementing an adaptive remeshing technique to the Delaunay triangulation algorithm. The adaptive remeshing technique places small elements around the crack tips and in regions with large changes of stress gradients. At the same time, larger elements are generated in other regions to minimize the total number of unknowns and the computational time. Several examples were employed to evaluate the combined Delaunay triangulation, the finite element method, and the adaptive remeshing technique. The combined procedure was used to predict the stress intensity factors for several geometries with different loadings, as well as to capture the crack growth trajectory. These examples demonstrated the capability of the combined adaptive Delaunay triangulation with the finite element method for solving crack propagation problems effectively.

Acknowledgements

The authors are pleased to acknowledge the Thailand Research Fund (TRF) for supporting this research work.

References

Anderson, T.L. (1991), *Fracture Mechanics: Fundamentals and Applications*, CRC Press, Florida.

ASTM 1996 (1996), *Annual Book of ASTM Standards*, American Society for Testing and Materials, Philadelphia.

Barsoum, R.S. (1977), "Triangular quarter-point elements as elastic and perfectly-plastic crack tip elements", *Int. J. Numer. Methods Eng.*, **11**, 85-98.

Bittencourt, T.N., Wawrzynek, P.A., Ingraffea, A.R. and Sousa, J.L. (1996), "Quasi-automatic simulation of crack propagation for 2D LEFM problems", *Eng. Fract. Mech.*, **55**, 321-334.

Borouchaki, H. and George, P.L. (1997), "Aspects of 2-D Delaunay mesh generation", *Int. J. Numer. Methods Eng.*, **40**, 1957-1975.

Bowyer, A. (1981), "Computing Dirichlet tessellations", *Comp. J.*, **24**(2), 162-166.

Chan, S.K., Tuba, I.S. and Wilson, W.K. (1970), "On the finite element method in linear fracture mechanics", *Eng. Fract. Mech.*, **2**, 1-17.

Dechaumphai, P. (1996), "Improvement of plane stress solutions using adaptive finite elements", *J. Chin. Inst. Eng.*, **19**, 375-380.

Erdogan, F. and Sih, G.C. (1963), "On the crack extension in plates under plane loading and transverse shear", *J. Basic Eng.*, **85**, 519-527.

Frey, W.H. (1987), "Selective refinement: a new strategy for automatic node placement in graded triangular meshes", *Int. J. Numer. Methods Eng.*, **24**, 2183-2200.

Guinea, G.V., Planas, J. and Elices, M. (2000), "K_I evaluation by the displacement extrapolation technique", *Eng. Fract. Mech.*, **66**, 243-255.

Isida, M. (1971), "Effect of width and length on stress intensity factors of internally cracked plates under various boundary conditions", *Int. J. Fract.*, **7**, 301-316.

Karamete, B.K., Tokdemir, T. and Ger, M. (1997), "Unstructured grid generation and a simple triangulation algorithm for arbitrary 2-D geometries using object oriented programming", *Int. J. Numer. Methods Eng.*, **40**, 251-268.

Lawson, C.L. (1977), *Software for C^1 Surface Interpolation. Mathematical Software III*, Academic Press, New York.

Peraire, J., Vahdati, M., Morgan, K. and Zienkiewicz, O.C. (1987), "Adaptive remeshing for compressible flow computations", *J. Comput. Phys.*, **72**, 449-466.

Phongthanapanich, S. and Dechaumphai, P. (2002), *Underwater Explosion Simulation by Transient Adaptive Delaunay Triangulation Meshing Technique*, Technical Report submitted to the Royal Thai Navy, TR-3894. Bangkok.

Rao, B.N. and Rahman, S. (2000), "An efficient meshless method for fracture analysis of cracks", *Comput. Mech.*, **26**, 398-408.

Sloan, S.W. (1993), "A fast algorithm for generating constrained Delaunay triangulations", *Comp. Struct.*, **47**, 441-450.

Watson, D.F. (1981), "Computing the *n*-dimensional Delaunay tessellation with application to Voronoi polytopes", *Comp. J.*, **24**(2), 167-172.

Weatherill, N.P. and Hassan, O. (1994), "Efficient three-dimension Delaunay triangulation with automatic point creation and imposed boundary constraints", *Int. J. Numer. Methods Eng.*, **37**, 2005-2039.

Zienkiewicz, O.C. and Taylor, R.L. (2000), *Finite Element Method*, Fifth Edition, Butterworth-Heinemann, Woburn.